Thermodynamic Analysis of the Phase Separation during the Polymerization of a Thermoset System into a Thermoplastic Matrix. I. Effect of the Composition on the Cloud-Point Curves

CARMEN CRISTINA RICCARDI,[1] JULIO BORRAJO,[1] LAURE MEYNIE,[2] FRANÇOISE FENOUILLOT,[2] JEAN-PIERRE PASCAULT[2]

[1]Institute of Materials Science and Technology, University of Mar del Plata and National Research Council, J. B. Justo 4302, B7608FDQ Mar del Plata, Argentina

[2]Laboratoire des Matériaux Macromoléculaires, UMR-CNRS 5627, Institut National des Sciences Appliquées, 17 Avenue Jean Capelle, 69 621 Villeurbanne Cedex, France

Received 24 September 2003; revised 3 November 2003; accepted 10 November 2003

ABSTRACT: The cloud-point curves of polystyrene (PS) mixed with reactive epoxy monomers based on diglycidyl ether of bisphenol A with stoichiometric amounts of 4,4′-methylenebis(2,6-diethylaniline) were experimentally studied. A thermodynamic analysis of the phase-separation process in these epoxy-modified polymers was performed that considered the composition dependence of the interaction parameter, $\chi(T,\Phi_2)$ (where T is the temperature and Φ_2 is the volume fraction of polystyrene), and the polydispersity of both polymers. In this analysis, $\chi(T,\Phi_2)$ was considered the product of two functions: one depending on the temperature [$D(T)$] and the other depending on the composition [$B(\Phi_2)$]. For mixtures without a reaction, the cloud-point curves showed upper critical solution temperature behavior, and the dependence of $\chi(T,\Phi_2)$ on the composition was determined from the threshold point, that is, the maximum cloud-point temperature. During the isothermal reactions of mixtures with different initial PS concentrations, the dependence of $\chi(T,\Phi_2)$ on the composition was determined under the assumption that, at each conversion level, the $D(T)$ contribution to the $\chi(T,\Phi_2)$ value had to be constant independently of the composition. For these mixtures, it was demonstrated that the changes in the chemical structure produced by the epoxy–amine reaction reduced $\chi(T,\Phi_2)$. This effect was more important at lower volume fractions of PS. Nevertheless, the decrease in the absolute value of the entropic contribution to the free energy of mixing was the principal driving force behind the phase-separation process. © 2003 Wiley Periodicals, Inc. J Polym Sci Part B: Polym Phys 42: 000–000, 2004

Keywords: phase separation; epoxy-modified polystyrene; composition dependence of the interaction parameter; polydisperse polymers

AQ: 3

INTRODUCTION

Thermoset/thermoplastic blends are materials resulting from the mixing of a thermoplastic polymer with the monomers precursors of a thermoset polymer and the subsequent curing reaction. Usually, the initial mixture is homogeneous, and because of the molar mass increase of the thermoset, a liquid–liquid phase separation occurs at a certain level of conversion.[1] Polymerizing a thermoset into a thermoplastic matrix is a new processing route for high-temperature-resistant

---

Correspondence to: C. C. Riccardi (E-mail: criccard@fi.mdp.edu.ar)

Journal of Polymer Science: Part B: Polymer Physics, Vol. 42, 000–000 (2004)

Table 1. Characteristics of the Different Reactants

Products	Formula	M^{n} (g mol^{-1})	M_{w} (g mol^{-1})	T_{g} (°C)	ρ (g cm^{-3})
DGEBA (n = 0.15; Bakelite)	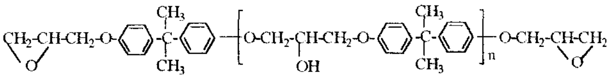	382.6		−27	1.15
MDEA (Lonza)	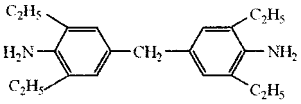	310.5			1.35
Lacqrene PS 1450N (Atofina)	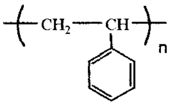	163,000	325,000	100	1.04

thermoplastic polymers.[2,3] The ultimate properties of these materials depend on the morphologies generated during curing. To predict or explain morphologies and properties, we must begin with a reasonable thermodynamic description of the system.

The lattice theory of Flory[4] and Huggins[5] is the best known theory used to describe the phase separation of polymeric solutions. Koningsveld and Kleintjens[6] extended this model to polydisperse polymer systems in which the Flory parameter was composition-dependent. Although this model was applied to solutions of polydisperse polymers with a constant molar mass distribution,[7–10] the distribution of the species generated during the polymerization of a thermosetting polymer was not considered. In previous works,[11–14] the Flory–Huggins approach, taking the polydispersity of both components into account (i.e., a constant molar mass distribution of the thermoplastic and a distribution varying with conversion for the thermoset), was used. The aim of the first part of this work is to show the application of the Koningsveld approach, which takes the polydispersity of the components into account, to experimental cloud-point curves of a model system, a polystyrene (PS)/epoxy–amine blend, through the determination of how the interaction parameter χ depends on the composition and temperature. Because the resulting thermodynamic model consists of three equations with four unknowns and the experimental phase volume ratio method[15] used to determine the critical point is inapplicable to this kind of blend, the composition dependence of χ is determined from the experimental threshold point for mixtures without a reaction and from the constancy of the temperature dependence of χ for mixtures reacting at a constant temperature.

In the second part of this work, the evolution of the volume fractions and the composition of the dispersed phase for a blend with 60 mass % PS is modeled with the developed thermodynamic model and is used to predict the evolution of the thermal properties.

EXPERIMENTAL

Materials

The epoxy system consisted of diglycidyl ether of bisphenol A (DGEBA; polydispersity index = 0.15) cured with 4,4′-methylenebis(2,6-diethylaniline) (MDEA). This system has already been described elsewhere.[16] The thermoplastic polymer used in this study was an amorphous PS supplied by Atofina. The chemical structures and characteristics of the reactants are listed in Table 1. T1

Blend Preparation

Blends were prepared with a two-step process. PS was first dissolved at 170 °C in DGEBA, and a stoichiometric amount of MDEA was dissolved in a second step at the same temperature. After 5 min of mixing, the material was removed from the mixer. The extent of the epoxy–amine reaction was negligible during the mixing procedure, and this was confirmed experimentally with differential scanning calorimetry (DSC).

Cloud-Point Curves

Quasibinary blends with different initial concentrations were formulated with a polydisperse PS (pseudocomponent 2) and DGEBA–MDEA stoichiometric mixture (pseudocomponent 1). The cloud-point temperatures (T_{CP}'s) of unreacted mixtures, containing different PS concentrations, were determined with a light transmission device[17] through a reduction in the temperature. T_{CP} was determined at the onset time of the light transmission decrease.

The polycondensation of reactive mixtures was carried out in the light transmission device at 177 °C. The cloud-point time was determined at the onset of the light transmission decrease. At this time, the test tube was taken out of the device and chilled in ice. The cloud-point conversion (p_{cp}) was determined with DSC. DSC analyses were conducted with a Mettler TA3000 apparatus under an argon atmosphere. The experiments were carried out from -100 to 350 °C at a heating rate of 10 °C/min. The conversion of epoxy groups (p) at time t is given by $p = 1 - \Delta H(t)/\Delta H_0$, where ΔH_0 is the total enthalpy of the reaction of the initial monomer mixture and $\Delta H(t)$ is the complementary enthalpy measured for a partially converted system at time t. ΔH_0 was also measured by DSC and was equal to 324 J/g.

Morphology of the Blends

For unreacted mixtures containing different PS concentrations, as soon as the separation occurred, the tubes were quenched in ice water to stop the epoxy–amine reaction. The morphology of the resulting biphasic blends was studied by transmission electron microscopy with a Philips CM 120. The samples were ultramicrotomed at room temperature and then vapor-stained with ruthenium tetroxide (RuO_4). The epoxy appeared light gray, whereas PS was dark.

THERMODYNAMIC ANALYSIS

Model

For a fluid mixture of two polydisperse polymers, with volume fractions given by

$$\Phi_1 = \sum_{i=1}^{m} \phi_i \quad \text{and} \quad \Phi_2 = \sum_{j=1}^{n} \phi_j \qquad (1)$$

Koningsveld and Kleintjens[6] expressed the Gibbs free energy change of mixing in terms of a g function as follows:

$$\frac{\Delta G}{MRT} = \sum_{i=1}^{m} \frac{\phi_i}{Z_i} \ln \phi_i + \sum_{j=1}^{n} \frac{\phi_j}{Z_j} \ln \phi_j + g\Phi_1\Phi_2 \qquad (2)$$

where M is the total number of lattice sites; R is the ideal gas constant; T is the absolute temperature; ϕ_i and ϕ_j are volume fractions of the i-mer and j-mer, respectively; and Z_i and Z_j are the number of lattice sites occupied by them. The residual Gibbs free energy, $g = g(T,\Phi_2)$ (where Φ_2 is the volume fraction of PS), is a function of the temperature and composition.

The chemical potentials μ_i and μ_j can be obtained from eq 2 by the usual procedures:

$$\frac{\Delta\mu_i}{RT} = \frac{\partial\left(\dfrac{\Delta G}{RT}\right)}{\partial n_i}\Bigg|_{P,T,n_{\neq i}} \quad \text{and} \quad \frac{\Delta\mu_j}{RT} = \frac{\partial\left(\dfrac{\Delta G}{RT}\right)}{\partial n_j}\Bigg|_{P,T,n_{\neq j}} \qquad (3)$$

That is,

$$\Delta\mu_i = RT\left[1 + \ln \phi_i - Z_i\left(\sum_{i=1}^{m} \frac{\phi_i}{Z_i} + \sum_{j=1}^{n} \frac{\phi_j}{Z_j}\right) + Z_i\Phi_2^2(g - g'\Phi_1)\right] \qquad (4)$$

$$\Delta\mu_j = RT\left[1 + \ln \phi_j - Z_j\left(\sum_{i=1}^{m} \frac{\phi_i}{Z_i} + \sum_{j=1}^{n} \frac{\phi_j}{Z_j}\right) + Z_j\Phi_1^2(g + g'\Phi_2)\right] \qquad (5)$$

where g' is the first derivate of g with respect to the composition Φ_2. By comparing eq 4 with the corresponding equation that arises from the Flory–Huggins model, we find that

$$\chi(T, \Phi_2) = g - g'\Phi_1 \qquad (6)$$

By integrating

$$\int_{\Phi_2}^{1} \chi(T,\, \Phi_2)\, d\Phi_2 = \int_{\Phi_2}^{1} g\, d\Phi_2 - \int_{\Phi_2}^{1} (1 - \Phi_2)\, dg \tag{7}$$

where $dg = g' d\Phi_2$, we obtain

$$(1 - \Phi_2)g = \Phi_1 g = \int_{1}^{\Phi_2} \chi(T,\, \Phi_2)\, d\Phi_2 \tag{8}$$

Replacing eqs 4 and 5, we obtain

$$\Delta\mu_i = RT\left[1 + \ln \phi_i - Z_i\left(\sum_{i=1}^{m} \frac{\phi_i}{Z_i} + \sum_{j=1}^{n} \frac{\phi_j}{Z_j}\right) + Z_i \Phi_2^2 \chi(T,\, \Phi_2)\right] \tag{9}$$

$$\Delta\mu_j = RT\left[1 + \ln \phi_j - Z_j\left(\sum_{i=1}^{m} \frac{\phi_i}{Z_i} + \sum_{j=1}^{n} \frac{\phi_j}{Z_j}\right) + Z_j\left(\int_{\Phi_2}^{1} \chi(T,\, \Phi_2)\, d\Phi_2 - \chi(T,\, \Phi_2)\Phi_1\Phi_2\right)\right] \tag{10}$$

$\chi(T,\Phi_2)$ is defined as the product of a temperature-dependent term [$D(T)$] and a concentration-dependent term [$B(\Phi_2)$]:[7–10]

$$\chi = D(T)B(\Phi_2) \tag{11}$$

$$\chi = \left(d_0 + \frac{d_1}{T}\right) \frac{1}{1 - b\Phi_2} \tag{12}$$

where d_0, d_1, and b are adjustable model parameters for a given system. The $D(T)$ and $B(\Phi_2)$ terms adopted in this work are the simplest ones.[18] If g is independent of the concentration [i.e., $B(\Phi_2) = 1$], it is equal to the χ parameter of the Flory–Huggins model.[4,5]

At the cloud point, there are two phases in equilibrium, α and β, and the well-known Gibbs law applies:[19,20]

$$\Delta\mu_i^{\alpha} = \Delta\mu_i^{\beta} \quad \text{and} \quad \Delta\mu_j^{\alpha} = \Delta\mu_j^{\beta} \tag{13}$$

The combination of these equations with eqs 9 and 10 and eqs 11 and 12 yields equations for the separation factors, σ_1 and σ_2:

$$\sigma_1 = \frac{1}{Z_i} \ln \frac{\phi_i^{\beta}}{\phi_i^{\alpha}} = \left(\sum_{i=1}^{m} \frac{\phi_i^{\beta}}{Z_i} + \sum_{j=1}^{n} \frac{\phi_j^{\beta}}{Z_j}\right) - \left(\sum_{i=1}^{m} \frac{\phi_i^{\alpha}}{Z_i} + \sum_{j=1}^{n} \frac{\phi_j^{\alpha}}{Z_j}\right) + D(T)\left(\frac{\Phi_2^{\alpha^2}}{1 - b\Phi_2^{\alpha}} - \frac{\Phi_2^{\beta^2}}{1 - b\Phi_2^{\beta}}\right) \tag{14}$$

$$\sigma_2 = \frac{1}{Z_j} \ln \frac{\phi_j^{\beta}}{\phi_j^{\alpha}} = \left(\sum_{i=1}^{m} \frac{\phi_i^{\beta}}{Z_i} + \sum_{j=1}^{n} \frac{\phi_j^{\beta}}{Z_j}\right) - \left(\sum_{i=1}^{m} \frac{\phi_i^{\alpha}}{Z_i} + \sum_{j=1}^{n} \frac{\phi_j^{\alpha}}{Z_j}\right) + D(T)\left(\frac{1}{b} \ln \frac{1 - b\Phi_2^{\alpha}}{1 - b\Phi_2^{\beta}} + \frac{\Phi_1^{\beta}\Phi_2^{\beta}}{1 - b\Phi_2^{\beta}} - \frac{\Phi_1^{\alpha}\Phi_2^{\alpha}}{1 - b\Phi_2^{\alpha}}\right) \tag{15}$$

where ϕ_i^{β} is equal to $\phi_i^{\alpha}\ \exp(\sigma_1 Z_i)$ and ϕ_j^{β} is equal to $\phi_j^{\alpha}\ \exp(\sigma_1 Z_j)$. At the beginning of the phase-separation process, the composition of the α phase is the initial one, and the composition of the β phase fulfills the balance:

$$\Phi_1^{\beta} + \Phi_2^{\beta} = 1 \tag{16}$$

Polymer Distribution Functions

The molar mass distribution of polymer 2 (PS) can be obtained with a Schulz–Zimm equation:[21]

$$w(j) = \left[\frac{f^{h+1}}{\Gamma(h + 1)}\right] j^{h} e^{-fj} \tag{17}$$

where $w(j)$ is the mass fraction of the j-mer, h is equal to $[\bar{x}_w/\bar{x}_n]^{-1}$, f is equal to $h/\bar{x}_n$, and Γ is the gamma function. For this PS, $\bar{x}_n$ is 1567, $\bar{x}_w$ is 3125, h is 1.006, and f is 6.42×10^{-4}. The concentrations of PS are expressed as volume fractions (ϕ_j) obtained from the densities shown in Table 1 under the assumption that the total volume did not change upon mixing.

For thermoset polymer 1, it is assumed that the DGEBA–MDEA reaction can be simulated by an ideal A_4–B_2 polycondensation (equal reactivity of functionalities, no substitution effects, and no intramolecular cycles in finite species). The main discrepancy with the actual distribution is caused by the fact that, in an aromatic diamine, the secondary amine reacts with a lower rate than the primary amine. The influence of this effect on the molar mass distribution is neglected.[14]

The molar concentration of generic $E_{H,K}$ species, containing H MDEA and K DGEBA molecules, at an overall conversion of p, is given by the Stockmayer distribution function:[22,23]

$$[E_{H,K}] = [\text{MDEA}]_0 \frac{4(3H)!p^{H+K-1}(1-p)^{2H+2}}{H!(3H-K+1)!(K-H+1)!} \tag{18}$$

where $[\text{MDEA}]_0$ is the initial molar concentration of the diamine.

The volume fraction of an $E_{H,K}$ species in the mixture is given by

$$\begin{aligned} \phi_i = \phi_{H,K} &= \lfloor E_{H,K} \rfloor V_{H,K} \\ &= [E_{H,K}]\left[H\frac{M_{\text{MDEA}}}{\rho_{\text{MDEA}}} + K\frac{M_{\text{DGEBA}}}{\rho_{\text{DGEBA}}}\right] \end{aligned} \tag{19}$$

where $V_{H,K}$ is the molar volume of $E_{H,K}$.

To state the thermodynamic model, we must define a reference volume (V_r). As usual,[7–10] we take the molar volume of the smallest species, that is, the molar volume of the repetitive unit in the PS molecule: V_r = 100 cm^3 mol^{-1}. Therefore,

$$Z_j = j \quad \text{and} \quad Z_i = \frac{V_{H,K}}{V_r} \tag{20}$$

As all the cells in the lattice model are busy, we obtain

$$M = \sum_{i=1}^{m} N_i Z_i + \sum_{j=1}^{n} N_j Z_j \tag{21}$$

where N_i and N_j are the molar numbers of species of sizes Z_i and Z_j, respectively. Consequently, the corresponding volume fractions are defined as follows:

$$\phi_i = \frac{N_i Z_i}{\sum_{i=1}^{m} N_i Z_i + \sum_{j=1}^{n} N_j Z_j} \tag{22}$$

$$\phi_j = \frac{N_j Z_j}{\sum_{i=1}^{m} N_i Z_i + \sum_{j=1}^{n} N_j Z_j} \tag{23}$$

NUMERICAL SOLUTION

Mixtures Before the Reaction

Mixtures of different volume fractions of PS with the DGEBA–MDEA pseudocomponent were selected. Before the reaction, experimental T_{CP}'s versus Φ_2 were obtained. For the calculation of the cloud-point curve, there are three equations (eqs 14, 15, and 16) to be solved for four unknowns [σ_1, σ_2, $D(T)$, and b]. To avoid this difficulty, we can obtain the b value from a critical point thermodynamic analysis. At the critical point, both the spinodal condition (the determinant of the second composition derivatives of the Gibbs free energy) and the neutral equilibrium condition (the determinant of the third composition derivatives of the Gibbs free energy) must be equal to zero. The rigorous expressions for spinodal and critical points, considering the composition dependence of the χ parameter along with the polydispersity of polymers, were derived by Koningsveld and Staverman:[24]

$$\begin{aligned} \frac{1}{\overline{Zw_1}\Phi_1} + \frac{1}{\overline{Zw_2}\Phi_2} - 2g + 2g'(1-2\Phi_2) \\ + g''\Phi_2(1-\Phi_2) = 0 \end{aligned} \tag{24}$$

$$\begin{aligned} \frac{\overline{Zz_1}}{\overline{Zw_1}^2\Phi_1^2} + \frac{\overline{Zz_2}}{\overline{Zw_2}^2\Phi_2^2} - 6g' + 3g''(1-2\Phi_2) \\ + g'''\Phi_2(1-2\Phi_2) = 0 \end{aligned} \tag{25}$$

where $\overline{Zw_1}$ and $\overline{Zw_2}$ and $\overline{Zz_1}$ and $\overline{Zz_2}$ are the corresponding weight and z size averages of polymers 1 and 2, respectively, and g', g'', and g''' are the first, second, and third composition derivates of the residual Gibbs free energy, $g(T, \Phi_2)$.

By considering eqs 6, 8, and 12, we find the following:

$$\frac{1}{\overline{Zw_1}\Phi_1} + \frac{1}{\overline{Zw_2}\Phi_2} - \frac{D(T)}{1-b\Phi_2}\left(\frac{b\Phi_2}{1-b\Phi_2} + 2\right) = 0 \tag{26}$$

$$\begin{aligned} \frac{\overline{Zz_1}}{\overline{Zw_1}^2\Phi_1^2} + \frac{\overline{Zz_2}}{\overline{Zw_2}^2\Phi_2^2} - \frac{D(T)b}{(1-b\Phi_2)^2} \\ \times\left(3 + \frac{2b\Phi_2}{1-b\Phi_2}\right) = 0 \end{aligned} \tag{27}$$

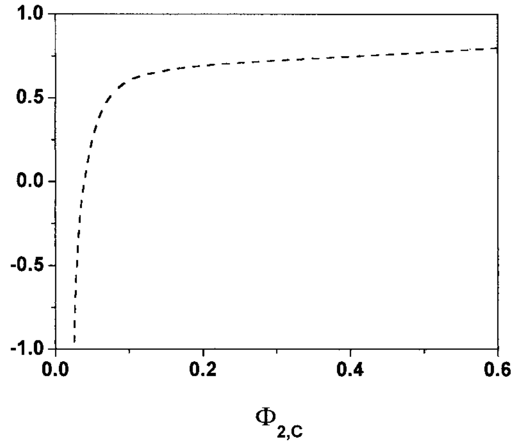

Figure 1. *b* value arising from spinodal and critical point criteria.

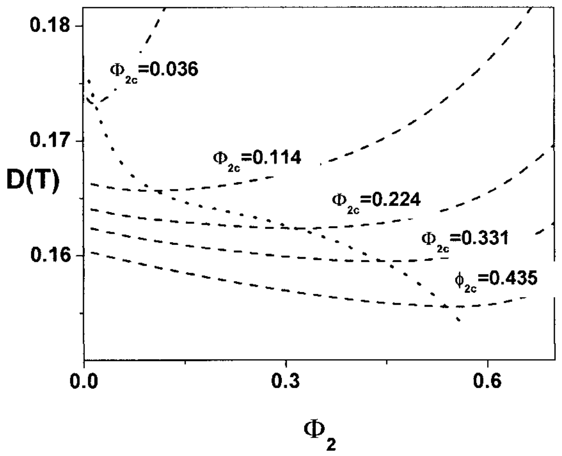

Figure 3. Effect of changes in $\Phi_{2,c}$ on cloud-point curves.

If the critical point can be determined experimentally, the critical value of $D(T)$ and the *b* value can be obtained from eqs 26 and 27. In this case, the equal phase volume criteria[15] for the critical point determination will be difficult to obtain experimentally because the mixture is highly viscous. As an alternative, we can determine the *b* value from the following analysis, knowing the experimental threshold temperature and composition on the measured cloud-point curve. Figure 1 shows the *b* values that make zero eqs 26 and 27 for different critical volume fractions of PS ($\Phi_{2,c}$), and Figure 2 shows the corresponding critical $D(T)$ values. From these figures, we can conclude that when $\Phi_{2,c}$ is increased, *b* increases and $D(T)_c$ decreases.

The numerical calculation of the cloud-point curves for different $\Phi_{2,c}$ values (i.e., different *b* values), expressed as $D(T)$ versus Φ_2, is shown in Figure 3. The minimum $D(T)$ value is shifted to the right, whereas $\Phi_{2,c}$ increases. The points of the minimum $D(T)$ value are the points of the maximum temperature because this system has upper critical solution temperature behavior and the $D(T)$ function is inversely proportional to T; therefore, the composition of the minimum $D(T)$ value is the composition of the threshold point. The dotted line in Figure 3 joins the points of the minimum $D(T)$ value, and knowing the experimental value of the composition for the threshold temperature, we can determine $\Phi_{2,c}$ from Figure 3 and the corresponding value of *b* from Figure 1.

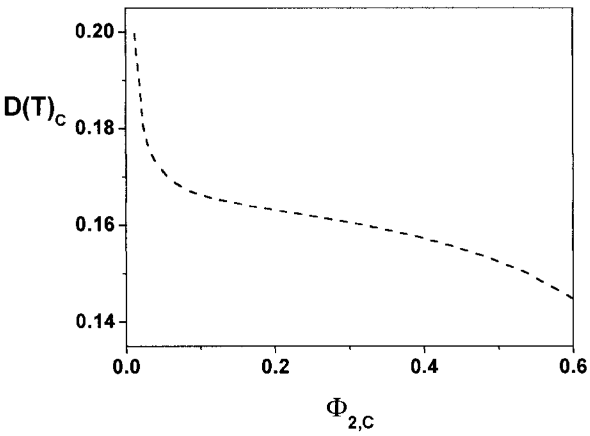

Figure 2. $D(T)_c$ versus $\Phi_{2,c}$.

Mixtures During Polycondensation

An experimental cloud-point-conversion curve, *p* versus Φ_2, was determined at a constant temperature of 177 °C during the reaction of mixtures of PS and DGEBA–MDEA under stoichiometric conditions with different initial concentrations. As for the mixtures without a reaction, for the calculation of the cloud-point curve, there are three equations (eqs 14, 15, and 16) with four unknowns [σ_1, σ_2, $D(T)$, and *b*]. Now the strategy consists of thinking that for a certain level of *p*, at a constant temperature, there will be a *b* value that makes $D(T)$ independent of the composition. For different levels of *p*, between 0 and 0.4, we have calculated $D(T)$ for the different compositions in the range of the experimental values by supposing *b* values. For each level of *p*, *b* has been selected if it gives the minimum standard devia-

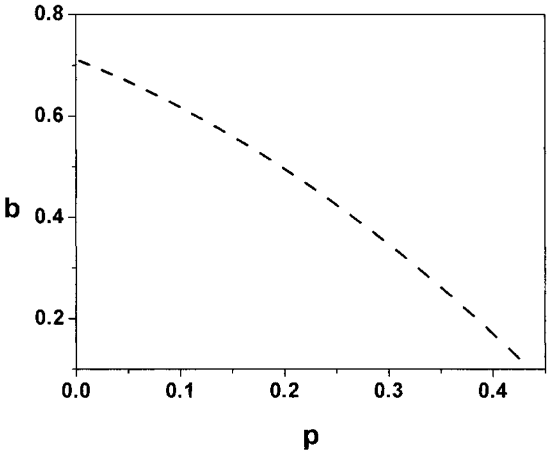

Figure 4. *b* versus *p*.

tion from the mean value of $D(T)$ versus the composition. From this analysis, the relationship between b and p has been determined and is plotted in Figure 4. F4

RESULTS AND DISCUSSION

Mixtures before the Reaction

Table 2 shows the experimental values of T_{CP} versus Φ_2. T2 The threshold point corresponds to $\Phi_2 = 0.435$. From Figure 3, the critical point is $\Phi_{2,c} = 0.331$, and from Figure 1, the corresponding b value is 0.732. The composition range for the phase inversion can be determined experimentally through an analysis of pictures of the morphology of the unreacted mixtures. Figure 5(a) shows that below 30 wt % PS, the matrix is epoxy, and Figure 5(b) shows that at this composition, $\Phi_{2,c} = 0.331$, the morphology is very close to the cocontinuity. F5

Table 2. T_{cp} Values of Mixtures before the Reaction

Φ_2	T_{cp} (°C)
0.05731	82.0
0.09128	83.0
0.11375	86.0
0.16933	85.0
0.22408	98.0
0.27801	105.5
0.33114	109.0
0.38348	110.0
0.43506	110.5
0.53600	98.0
0.63407	92.0

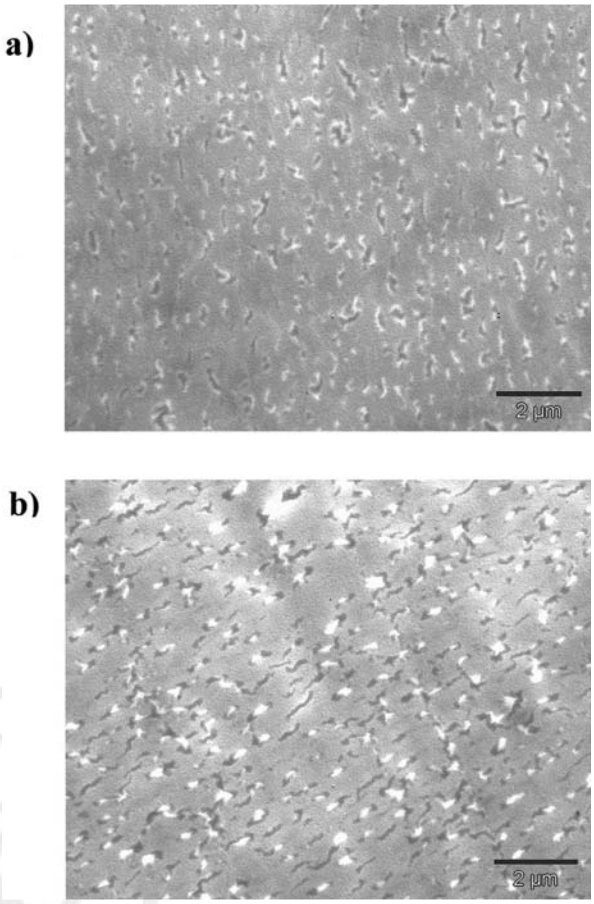

Figure 5. Morphology of unreacted PS/DGEBA–MDEA blends: (a) 25/75 (w/w) and (b) 30/70 (w/w). AQ: 4

Cloud-point curves were calculated with eqs 14, 15, and 16 according to the procedure devel-

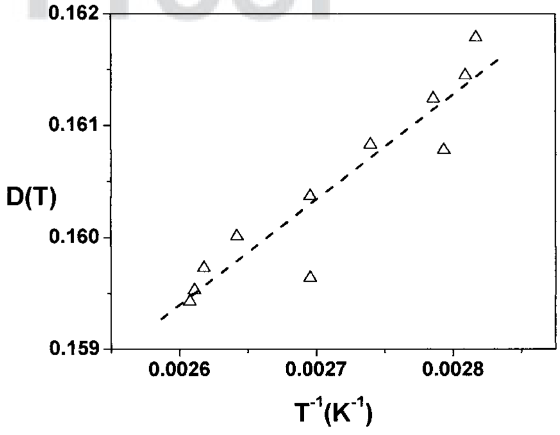

Figure 6. $D(T)$ versus the reciprocal of the temperature (T^{-1}). AQ: 5

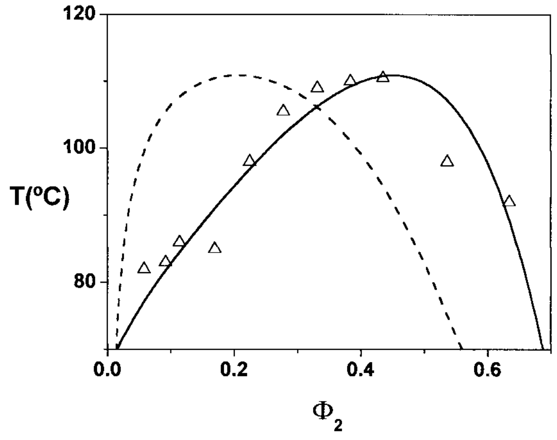

Figure 7. (—) Cloud-point and (–) shadow curves for mixtures without the reaction. The triangles represent experimental points.

oped by Kamide et al.,[25] and the obtained $D(T)$ values were correlated with the temperature.
F6 From Figure 6, we find that

$$D(T)|_{p=0} = 0.13493 + \frac{9.4111}{T(\mathrm{K})} \tag{28}$$

Figure 7 shows cloud-point and shadow curves calculated for mixtures without a reaction along
F7 with the experimental cloud-point data.

If we assume that χ is independent of the composition (i.e., $b = 0$), calculated $D(T)$ values from the experimental cloud-point curve cannot be correlated with the temperature, as shown in
F8 Figure 8.

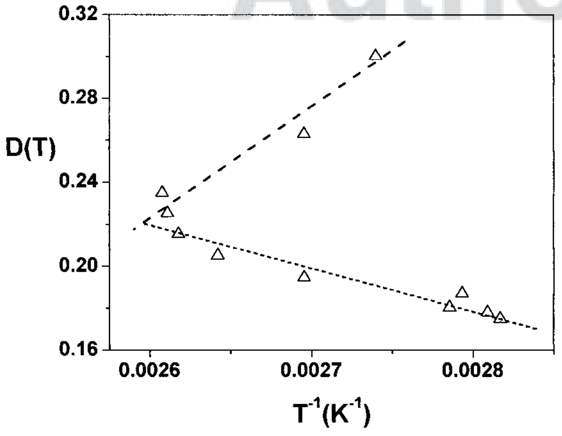

Figure 8. Temperature dependence of χ if the composition dependence is not taken into account.

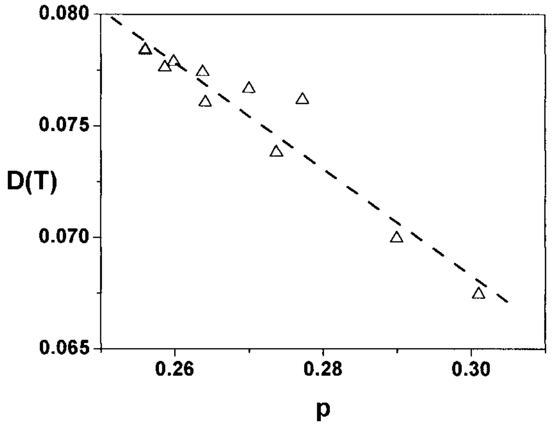

Figure 9. $D(T)$ versus p.

Mixtures during Polycondensation

From Figure 4, the following phenomenological expression has been obtained:

$$b = 0.7120 - 0.0809p - 1.3610p^2 \tag{29}$$

Similarly, Choi and Bae[10] showed that b decreased as the molar mass of PS increased in a mixture of PS and cyclohexane. The extrapolated value of b for $p = 0$ (i.e., 0.7120) differs by only 2.7% from that determined previously from the experimental threshold temperature.

With this expression, cloud-point curves were calculated from eqs 14, 15, and 16, and the obtained D values were correlated with the conver-
sion. From Figure 9, we find F9

$$D|_{177\,^{\circ}\mathrm{C}} = 0.13985 - 0.23821p \tag{30}$$

As demonstrated in previous works,[13,14] χ decreases with conversion because of changes in the chemical structure and associated specific interactions. This favors PS miscibility in the reaction medium. This means that thermoset oligomeric species are more compatible with PS than the starting mixture of the monomers. This implies that miscibility is enhanced as the reaction proceeds; however, phase separation originates from the prevailing influence of the reduction in the entropic contribution to the free energy of mixing. To elucidate the difference between the $D(T)$ value extrapolated at 177 °C for a mixture before reaction and that arising from eq 30, we would determine cloud-point curves at different constant temperatures. Instead, we focus our attention on the results at 177 °C because, in the second part of this work, we analyze the evolution of the volume fraction and composition of the dispersed phase for a blend with 60 wt % PS at this temperature.

Figure 10 shows p_{cp} versus Φ_2, for the PS/DGEBA–MDEA system containing different PS volume fractions at 177 °C. F10

With the PS composition as a parameter in the range of 0.01–0.99, the effect of p on χ is shown in F11 Figure 11. Although p increases, χ decreases independently of the composition level, and this effect is more drastic for higher values of Φ_2 because of the relationship between b and p.

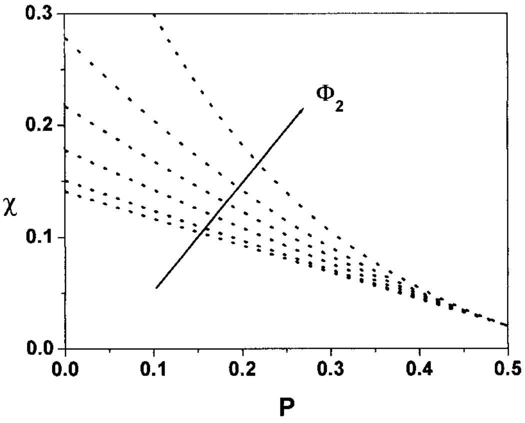

Figure 11. χ versus p.

CONCLUSIONS

A thermodynamic analysis of the phase-separation process in epoxy-modified PS was performed that considered the composition dependence of the χ parameter and the polydispersity of both the thermoplastic and epoxy–amine network in the formation.

For mixtures without a reaction, the cloud-point curve showed an upper critical solution temperature behavior, and the dependence of χ on the composition was determined from the threshold point.

For mixtures during the reaction, the dependence of χ on the composition was determined under the assumption that at each level of p, at a constant temperature, the D contribution to the χ value did not depend on the composition. For the PS/DGEBA–MDEA mixtures, it was demonstrated that χ decreased when the epoxy–amine reaction proceeded, that is, when the chemical structure of the species evolved. This effect was more important at lower volume fractions of PS. Notwithstanding the reduction of χ, the reduction of the absolute value of the entropic contribution to the free energy of mixing remained the principal driving force behind the phase-separation process.

In the second part of this work, the evolution of the volume fractions and the composition of the dispersed phase for a blend with 60 wt % PS are modeled with the developed thermodynamic model.

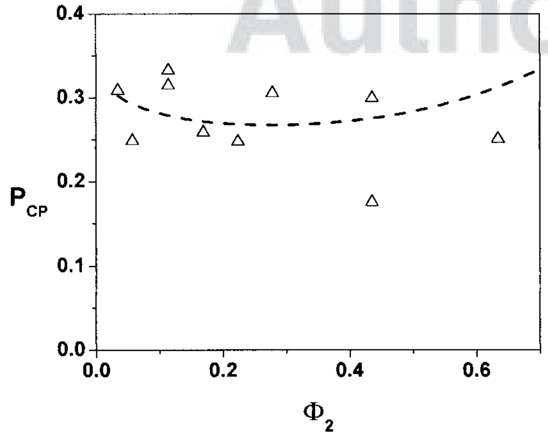

Figure 10. Cloud-point curve for mixtures during polycondensation. The triangles represent experimental points.

REFERENCES AND NOTES

1. Williams, R. J. J.; Rozemberg, B. A.; Pascault, J. P. Adv Polym Sci 1996, 128, 95.
2. Vanderbosh, R. W.; Meijer, H. E. E.; Lemstra, P. J. Polymer 1995, 36, 2903.
3. Lemstra, P. J.; Kurja, J.; Meijer, H. E. E. In Materials Science and Technology; Cahn, R. W.; Haasen, P.; Kramer, E. J.; Meijer, H. E. E., Eds.; Wiley-VCH: Weinheim, 1997; Vol. 18, p 513. AQ: 1
4. Flory, P. J. J Chem Phys 1942, 10, 21.
5. Huggins, L. J Phys Chem 1942, 46, 151.
6. Koningsveld, R.; Kleintjens, L. A. J Polym Sci 1977, 61, 221. AQ: 2
7. Qian, C.; Mumby, S. J.; Eichinger, B. E. Macromolecules 1991, 24, 1655.
8. Bae, Y. C.; Shim, J. J.; Soane, D. S.; Prausnitz, J. M. J Appl Polym Sci 1993, 47, 1193.
9. Bae, Y. C.; Lambert, D. S.; Soane, D. S.; Prausnitz, J. M. Macromolecules 1991, 24, 4403.
10. Choi, J. J.; Bae, Y. C. Fluid Phase Equilib 1999, 157, 213.

11. Riccardi, C. C.; Borrajo, J. Polym Int 1993, 32, 241.
12. Riccardi, C. C.; Borrajo, J.; Williams, R. J. J. Polymer 1994, 35, 5541.
13. Borrajo, J.; Riccardi, C. C.; Williams, R. J. J.; Cao, Z. Q.; Pascault, J. P. Polymer 1995, 36, 3541.
14. Riccardi, C. C.; Borrajo, J.; Williams, R. J. J.; Girard-Reydet, E.; Sautereau, H.; Pascault, J. P. J Polym Sci Part B: Polym Phys 1996, 34, 349
15. Krause, C.; Wolf, B. A. Macromolecules 1997, 30, 825.
16. Eloundou, J. P.; Ayina, O.; Ntede Nga, H.; Gerard, J. F.; Pascault, J. P.; Boiteux, G.; Seytre, G. J Polym Sci Part B: Polym Phys 1998, 36, 2911.
17. Moschiar, S. M.; Riccardi, C. C.; Williams, R. J. J.; Verchere, D.; Sautereau, H.; Pascault, J. P. J Appl Polym Sci 1991, 42, 717.
18. Kamide, K. In Thermodynamics of Polymer Solutions, Phase Equilibria and Critical Phenomena; Jenkins, A. D., Ed.; Polymer Science Library 9; Elsevier: New York, 1990; Chapter 4.
19. Flory, P. J. Principles of Polymer Chemistry; Cornell University Press: Ithaca, NY, 1953.
20. Kurata, M. Thermodynamics of Polymer Solutions; Harwood Academy: London, 1982; Chapter 2.
21. Peebles, L. H. Molecular Weight Distributions in Polymers; Wiley-Interscience: New York, 1971.
22. Stockmayer, W. H. J Polym Sci 1952, 9, 69.
23. Stockmayer, W. H. J Polym Sci 1953, 11, 424.
24. Koningsveld, R.; Staverman, A. J. J Polym Sci Part A-2: Polym Phys 1968, 6, 325.
25. Kamide, K.; Matsuda, S.; Shirataki, H. Eur Polym J 1990, 26, 379.

AQ1: Please confirm the reference as edited.

AQ2: Please provide the complete title of the journal.

AQ3: Please provide two more keywords from the common keyword catalog located at http://www.interscience.wiley.com/jpages/0887-6266/keyword.pdf.

AQ4: Please provide the original photograph or an EPS/TIFF file.

AQ5: Please confirm the legend as edited.